DOI: 10.1002/ejic.201100958

Exploring $(Ph_2PCH_2CH_2)_2E$ Ligand Space (E = O, S, PPh) in Rh^I Alkene Complexes as Potential Hydroacylation Catalysts

Sebastian D. Pike,[a] Rebekah J. Pawley,[a] Adrian B. Chaplin,[a] Amber L. Thompson,[a] Joel A. Hooper,[a] Michael C. Willis,[a] and Andrew S. Weller*[a]

Keywords: Rhodium / NMR spectroscopy / Phosphanes / Decarbonylation / Alkenes

The ligands $(Ph_2PCH_2CH_2)_2E$ (E = O, S, PPh) have been used to form a variety of Rh^I cations $[Rh\{(Ph_2PCH_2CH_2)_2E\}(alkene)]^+$ (alkene = methyl acrylate, trimethylvinylsilane). Variable-temperature NMR spectroscopy shows that the methyl acrylate ligands undergo a fluxional process on the metal, via a κ^1-carbonyl intermediate, while the trimethylvinylsilane complexes cannot access this intermediate and do not undergo the same process. Their reactivity in hydroacylation reactions with 1-pentanal have been investigated, and these studies further suggest the important role that a chelating substituent next to the aldehyde might play in productive hydroacylation.

Introduction

The transition-metal-catalysed hydroacylation reaction is one that couples alkenes (or alkynes) with aldehydes, in an atom-efficient way, to produce ketones [Equation (1), Scheme 1].[1–4] It has attracted significant attention in recent years, and a variety of, mainly rhodium-based, catalysts have been described. The mechanism proceeds through oxidative addition of aldehyde to a Rh^I centre to give an acyl–hydride, olefin binding, and migratory insertion followed by reductive elimination – which is accepted to be the turnover limiting step.[1,5–7] A significant obstacle barring the way to the wider implementation of this potentially powerful methodology is the competitive reductive decarbonylation reaction,[8,9] which produces an inactive metal carbonyl. This occurs from a low-coordinate acyl–hydride intermediate by (reversible) migratory deinsertion of CO to a *cis*-vacant site, followed by irreversible reductive elimination of a saturated product (R–H). Both productive (olefin coordination, product reductive elimination[10,11]) and unproductive (carbonyl deinsertion,[12,13] reductive elimination of R–H) steps require a low-coordinate transition-metal complex, and a number of strategies have been employed to promote the hydroacylation reaction over decarbonylation. In view of this, chelation control from the substrate,[2,3,14–16] by using, for example, β-S-substituted aldehydes such as **A** (Scheme 1),[17] is one of the strategies used to deliver successful intermolecular hydroacylation. Combined with this, we have also reported the use of a hemilabile[18] diphosphanylether ligand, DPEphos, to protect the vacant site on the metal centre towards decarbonylation, in which the central oxygen on the ligand can move away to allow for both olefin coordination and reductive elimination of the product.[19,20] With a ligand that does not act in a hemilabile manner, such as Xantphos or $(Ph_2PCH_2CH_2)_2O$, e.g. complex **B**, Scheme 1, β-S-substituted aldehydes undergo oxidative addition to give a six-coordinate complex that does not proceed to bind an olefin, as the central oxygen remains tightly bound. This stable six-coordinate configuration, however, does lead to complexes that are stable to decarbonylation.[21]

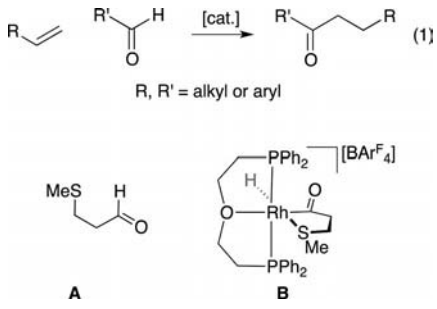

Scheme 1.

Milstein and co-workers have shown the stability of five-coordinate Rh^{III}–hydrido–acyl complexes towards decarbonylation can be controlled by the π-donor nature of the supporting ligands, which place the acyl group either *cis* or *trans* to a vacant site,[13] depending on the geometry of the five-coordinate intermediate. Similar observations have been made by Nolan and Goldman,[22] which also underscore computational work by Eisenstein on the relative geometries of d^6 ML_5 species.[23] We were thus particularly interested in exploring the reactivity of simple, non-chelating,

[a] Department of Chemistry, Inorganic Chemistry Laboratory, University of Oxford,
South Parks Road, Oxford, OX1 3QR, UK
E-mail: andrew.weller@chem.ox.ac.uk

aliphatic aldehydes with Rh^I complexes with tridentate ligands $(Ph_2PCH_2CH_2)_2E$ (E = S, O, PPh), in which the central donor atom changes from being a potential π-donor (E = O, S) to one that is not (E = PPh) (Scheme 2). Such complexes would give five-coordinate acyl–hydride intermediates on oxidative addition of simple aldehydes. To do this, Rh^I precursors that are set up for oxidative addition reactions are required, and we report cationic, alkene adducts $[Rh\{(Ph_2PCH_2CH_2)_2E\}(alkene)]^+$, as such complexes are also likely to be compatible with the overall catalytic cycle in which alkene is present in excess. We further describe the reactivity of these complexes with pentanal in the hydroacylation reaction with methyl acrylate. Related Rh^I complexes have been reported as aldehyde decarbonylation catalysts, albeit operating at elevated temperatures to facilitate turnover.[8,24,25]

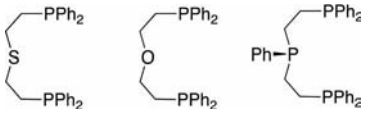

Scheme 2.

Results and Discussion

Synthesis

Our preparative route to the target complexes starts from simple halide precursors (Scheme 3). $[Rh\{(\kappa^3\text{-}Ph_2PCH_2CH_2)_2PPh\}Cl]$[26] was prepared by slight modifications to a known preparation, while $[Rh\{(\kappa^3\text{-}Ph_2PCH_2CH_2)_2S\}Cl]$ is a new complex prepared in good isolated yield by addition of free ligand[27] to $[Rh(cod)Cl]_2$. Addition of the alkenes, methyl acrylate or vinyltrimethylsilane, to CH_2Cl_2 solutions of these complexes in the presence of $Na[BAr^F_4]$, to abstract chloride, resulted in the rapid (30 min) and clean formation of the new complexes $[Rh\{(\kappa^3\text{-}Ph_2PCH_2CH_2)_2E\}(\eta^2\text{-}H_2C{=}CHR)][BAr^F_4]$ {E = S **1**, PPh **2**; R = C(O)OMe **a**, $SiMe_3$ **b**; Ar^F = C_6H_3-3,5-$(CF_3)_2$}. These were characterised by NMR spectroscopy, and for **2a** also by single-crystal X-ray diffraction as the $[B(3,5\text{-}Cl_2C_6H_3)_4]^-$ salt.[28] We have recently reported the in situ formation of $[Rh\{(\kappa^3\text{-}Ph_2PCH_2CH_2)_2O\}\{\eta^2\text{-}H_2C{=}CHC(O)OMe\}][BAr^F_4]$ (**3a**) by a different route,[21] but did not describe the solid-state structure. For comparison with **2a**, we also report that here. We were unable to prepare the vinyltrimethylsilane complex analogue of **3a** as in our hands, the complex $[Rh\{(\kappa^3\text{-}Ph_2PCH_2CH_2)_2O\}Cl]$ could not be prepared by a route similar to those for $[Rh\{(\kappa^3\text{-}Ph_2PCH_2CH_2)_2PPh\}Cl]or[Rh\{(\kappa^3\text{-}Ph_2PCH_2CH_2)_2S\}Cl]$, while alternative routes also did not work.[21]

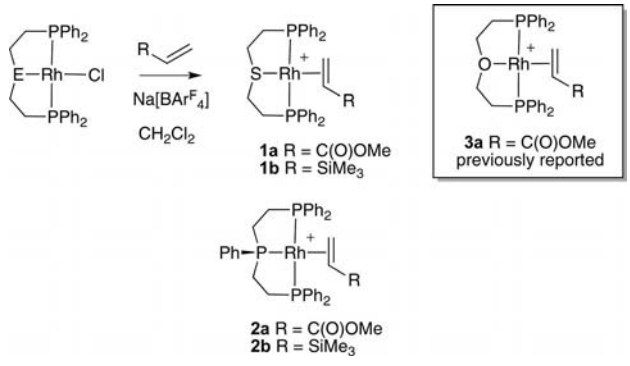

Scheme 3. ($[BAr^F_4]^-$ anions omitted for clarity).

Solid-State Structures

The solid-state structures of **2a** and **3a** (Figures 1 and 2) are broadly similar, both have pseudo-square-planar environments around the rhodium atom with similar Rh–P distances and a η^2-bound alkene. The structural refinement for **3a** was not as high quality as that for **2a** because of the nature of the crystals (see Experimental Section). For **3a**, the alkene is disordered over two positions in a 70:30 ratio, related to each other by an approximate reflection, to afford an enantiomeric pair of cations. The major difference between **2a** and **3a** comes from structural metrics associated with the bound methyl acrylate, which is orientated approximately in plane with respect to the RhP_3 plane in **2a** and upright for both components in **3a**. The C–C distance in the alkene in **2a** [1.381(3) Å] appears slightly shorter than those in **3a** [1.405(7) Å, major; 1.411(9) Å minor], although within error they are equivalent. These distances lie in the range found for later transition metals bound with methyl acrylate (≈1.3–1.43 Å).[29–31] The corresponding Rh–C distances are, however, statistically longer for **2a** than for **3a** [viz. 2.221(2), 2.219(2) vs. 2.074(16)–2.148(17) Å, respectively], which might suggest more back-donation from the metal to the alkene in **3a**. The orientation of alkene ligands in d^8 ML_3 fragments has received much attention, and studies indicate that steric factors tend to outweigh electronic factors associated with the back-donation from a suitable metal orbital to the alkene π* orbital,[32] which leads to upright alkene orientations and a small barrier to rotation of the alkene around the metal–alkene-axis. In-plane orien-

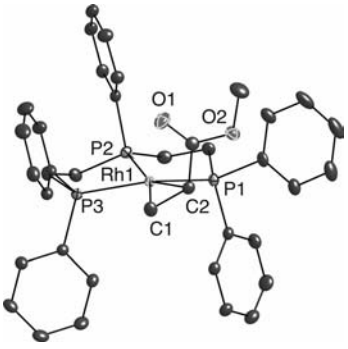

Figure 1. Solid-state structure of **2a**. Hydrogen atoms and anions omitted. Thermal ellipsoids at the 30% probability level. Selected bond lengths [Å] and angles [°]: **2a**: Rh–P1 2.2942(6), Rh–P2 2.2328(6), Rh–P3 2.3300(6), C1–C2 1.381(3), Rh–C1 2.221(2), Rh–C2 2.219(2); ∠ (torsion) C1C2/O1C3 –22.8(4); ∠ (planes) P3Rh1P1P2/Rh1C1C2 28.78(11).

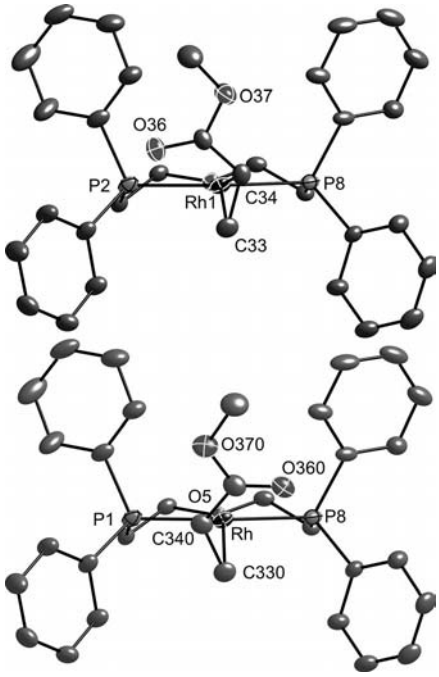

Figure 2. Solid-state structure of **3a** (minor component shown at bottom, ratio 70:30, respectively). Selected bond lengths [Å] and angles [°]: **3a**: Rh1–P2 2.2917(16), Rh1–P8 2.2982(16), Rh1–O5 22.100(3), C33–C34 1.405(7), Rh1–C33 2.074(16), Rh1–C34 2.144(7), C330–C340 1.411(9), Rh1–C330 2.11(4), Rh1–C340 2.148(17); ∠ (torsion) C33/C34/C35/O36 12.4(11)°, C330/C340/C350/O360 –11(3)°; ∠ (planes) O5Rh1P8P2/Rh1C33C34 76.9(5)°, O5Rh1P8P2/Rh1C330C340 69.6(12)°.

tations of the alkene are also known where subtle steric effects favour this conformation.[33] It would seem that these electronic and steric contributions are finely balanced in the systems here, with both orientations observed in the solid state (but likely share the same orientation in solution vide infra). However, it does appear that the upright orientation in **3a** allows for slightly better back-donation from the Rh^I centre to the alkene, which would be in line with a suitable high-lying, filled metal orbital that also has a contribution from the π-donor oxygen atom, similar to that calculated for analogous $\{Rh(PR_3)_2Cl\}$ fragments.[34] Surprisingly, there are only a handful of κ^3-$(Ph_2PCH_2CH_2)_2O$[21,35] or κ^3-$(Ph_2PCH_2CH_2)_2PPh$[8,26,36] structures reported with Rh, and none with $(Ph_2PCH_2CH_2)_2S$.

Solution NMR Spectroscopic Data

In solution at 298 K for complexes **1a** and **2a**, the $^{31}P\{^1H\}$ NMR spectroscopic data indicate one phosphorus environment for the two *trans*-related phosphanes (e.g. P_1/P_3 in **2a**) that also show coupling to ^{103}Rh, and for **2a**, an additional environment is observed that mutually couples to the two other *cis* phosphanes (P_2). In the ^1H NMR spectrum, peaks assigned to the bound alkene are observed, which are similar to those reported for **3a**,[21] e.g. **2a** δ = 3.07 ppm (1 H), δ = 4.04 ppm (1 H + 1 H coincidence). COSY and $^1H/^{13}C$ HSQC experiments were used to fully assign individual signals for **2a**, and by analogy those for **1a**. For **1a**, only two methylene environments (4 H relative integral each) are observed in contrast to the four observed for **2a** (and **3a**[21]).

These data suggest fluxional processes are occurring in solution to give time-averaged C_{2v} symmetry to the $\{Rh(PEP)\}^+$ fragment for **1a** and C_s symmetry for **2a** and **3a**. A simple rotation of the alkene around the Rh–C1/C2 vector would make the phosphanes equivalent, and give time-averaged C_{2v} symmetry, only if associated with a low-energy inversion of stereochemistry at the central E group.[37,38] The NMR spectroscopic data suggest that this occurs for **1a** (E = S) but not for **2a** or **3a**, which show only C_s symmetry. For **2a**, inversion at the central PPh is likely to be a high-energy process, while inversion at O in **3a** is also clearly not a low-energy process. Thus, in order to obtain the observed equivalence of the phosphanes in **2a** and **3a**, some other fluxional process must be occurring other than simple alkene rotation. The cooling of a sample of **1a** from room temperature to 200 K (CD_2Cl_2) results in NMR spectra that are consistent with a static structure, i.e. a tightly coupled AB doublet with inequivalent phosphorus environments in the $^{31}P\{^1H\}$ NMR spectrum. The outer lines of the second-order multiplet are of very low intensity and could not be resolved. At this temperature, the methylene signals are broad and do not offer any additional structural information. For **2a**, significant broadening is observed at 190 K in the $^{31}P\{^1H\}$ NMR spectrum, which suggests that the low-temperature limit is being approached. As for **1a**, the methylene signals are very broad in the ^1H NMR spectrum at low temperature and offer no extra information. For **3a**, however, progressive cooling results in a $^{31}P\{^1H\}$ NMR spectrum at 200 K that shows a clearly resolved AB doublet with a ^{31}P–^{31}P coupling constant of 384 Hz (Figure 3). In the ^1H NMR spectrum at this lowest temperature, the three alkene peaks all shift ca. 0.7 ppm to a lower frequency, and at least six broad environments are observed for the methylene protons of the POP ligand. These data are fully consistent with the static solid-state structure. The variable-temperature ^{31}P NMR spectroscopic

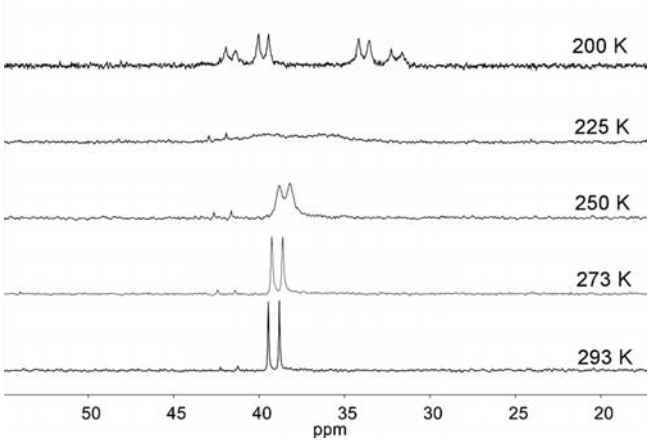

Figure 3. Variable-temperature $^{31}P\{^1H\}$ NMR spectra of **3a**. The signal at $\delta \approx 42$ is an unidentified minor impurity.

data are of sufficient quality to allow a line–shape analysis and an Eyring plot, from which the activation parameters of $\Delta H^{\ddagger} = +48 \pm 2\ kJ\,mol^{-1}$ and $\Delta S^{\ddagger} = +37 \pm 9\ JK^{-1}mol^{-1}$ were calculated [$\Delta G^{\ddagger}(298) = +37 \pm 5\ kJ\,mol^{-1}$]. Given that inversion of the phosphane ligand backbone is proposed to not be occurring in **3a**, these data indicate the barrier to the fluxional process of the alkene only. In the presence of excess alkene, no exchange was observed on the NMR timescale for **1a** or **2a**, with sharp peaks observed for both free and bound alkene. By contrast, **3a**, when prepared in situ, has been reported to show slow exchange with excess methyl acrylate.[21] Its isolation in the pure form here shows that it displays sharp ^1H NMR resonances for the bound alkene in the absence of excess methyl acrylate.

To explore this fluxional process in more detail, we prepared the vinyltrimethylsilane complexes $[Rh\{(\kappa^3\text{-}Ph_2PCH_2CH_2)_2E\}(\eta^2\text{-}H_2C{=}CHSiMe_3)][BAr^F{}_4]$ **1b** and **2b** by a similar route to that for **1a** and **2a**. We have not been able to prepare **3b**. The incorporation of a $SiMe_3$ group has a significant effect on the fluxional process. At room temperature, the $^{31}P\{^1H\}$ NMR spectrum for **1b** shows a very broad, almost featureless spectrum, and the ^1H NMR spectrum shows broad peaks for the methylene groups, but very sharp peaks for the coordinated vinyl trimethylsilane. No exchange is observed on addition of free alkene. On cooling (200 K), the alkene peaks do not change in position, but the methylene signals sharpen to give eight environments, and the $^{31}P\{^1H\}$ NMR spectrum shows a tightly coupled AB doublet [J(P,P) = 280 Hz]. The variable-temperature ^{31}P NMR spectroscopic data are of sufficient quality to allow an Eyring plot, from which the activation parameters of $\Delta H^{\ddagger} = +58 \pm 2\ kJ\,mol^{-1}$ and $\Delta S^{\ddagger} = +10 \pm 5\ JK^{-1}mol^{-1}$ were calculated [$\Delta G^{\ddagger}(298) = +55 \pm 4\ kJ\,mol^{-1}$]. This is the upper limit for alkene rotation/inversion at sulfur, and the measured activation parameters are consistent with those reported for other systems.[38] In contrast, **2b** shows sharp signals at room temperature, with eight methylene environments observed in the ^1H NMR spectrum. Three ^{31}P environments are observed, which all couple to one another, with two showing characteristic *trans* ^{31}P–^{31}P coupling [J(P,P) = 331 Hz]. These data are consistent with a high barrier to inversion at phosphorus.

The observation of broad signals for the methylene groups in **1b** suggests inversion at S is a higher barrier process than that in **1a**; but perhaps, most importantly, the observation of three sharp environments for the phosphanes in **2b** shows that there is no fluxional process operating to make two of them equivalent, unlike for **2a**. Pulling all these data together, we suggest two fluxional processes are occurring: (i) the inversion at S, which is rapid in **1a** but slower in **1b**; while for **2a** and **2b**, no such inversion is possible; (ii) a process that effectively flips the alkene in **2a**, but not **2b**, which is probably also operating in **3a**. This second process must be mediated by the acrylate group, as the $SiMe_3$ group effectively halts the process in **2b**. Given the small, but positive, entropy of activation measured for the fluxional process in **1a** and **3a**, coupled with the fact that exchange with free alkene is slow, at best, for **1a**–**3a**, we suggest an intramolecular mechanism that involves the alkene coordinating through the oxygen (intermediate **A**, Scheme 4), alkene flip around a nominal mirror plane, and re-coordination of the alkene. We discount alternative coordination modes of the alkene in the intermediate species **A**, such as η^2-CO:η^2-CC or a metallocyclic structure[39,40] as this would neither account for the positive entropy of activation nor the observed inequivalence of the geminal alkene protons. The two η^2-CC structures shown in Scheme 4 represent the two components of disorder observed in the solid state for **3a**.

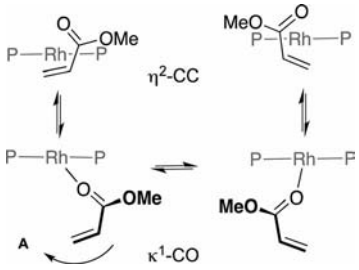

Scheme 4. Suggested mechanism for the fluxional process in complexes **1a**, **2a** and **3a**.

Reaction with Aldehydes

Having established the synthesis and structures of the Rh^I alkene precursors, we investigated the reactivity with pentanal. To our surprise, none of the complexes reacted with the aldehyde over an appreciable timeframe, with the unreacted alkene complex returned instead. Likewise, under catalytic conditions (10 mol-%), **1a**, **2a** and **3a** did not turnover methyl acrylate and pentanal, with only the alkene complexes observed. This lack of reactivity is in contrast with that of β-S-substituted aldehyde **A** with **3a**, which rapidly reacts by oxidative addition to give **B** (Scheme 1). Presumably, this reflects the requirement for an intermediate with a coordinated σ-aldehyde to form prior to oxidative addition,[41] and the alkenes are too tightly bound to be easily displaced by pentanal, while the sulfur tether in **A** is able to. Similar comments have been made with regard to the role of alkene in the intramolecular hydroacylation of 4-pentenal.[42] However, over extended time (2 d) solutions of **1a** and **3a** do react with pentanal and are converted smoothly to give the products of decarbonylation, **1c** and **3c** (Scheme 5).[35] Interestingly, **2c** was only observed as a minor product after a longer period of time, with **2a** still present as the major component, which suggests an even slower reaction with the aldehyde. Compound **2c** has previously been prepared as the $[SbF_6]^-$ salt by Crabtree.[8] Compound **1c** can be alternatively prepared in the absence of olefin by the rapid reaction of $[Rh\{(\kappa^3\text{-}Ph_2PCH_2CH_2)_2S\}Cl]$ with $Na[BAr^F{}_4]$ as a halide abstracting reagent in the presence of pentanal at room temperature. This demonstrates that under suitable conditions (i.e. no alkene) oxidative addition of the aldehdye, followed by rapid reductive decarbonylation, can occur. Pertinently, **2c** is formed much

more slowly by the analogous preparation from [Rh{(κ^3-$Ph_2PCH_2CH_2)_2PPh$}Cl] (50% conversion after 11 d), with a hydride species initially formed: δ^1H = –19.70 ppm [ddt, $J(P_2H)$ = 37, $J(P_{1,3}H)$ = 12, J(RhH) = 22 Hz]; $\delta^{31}P\{^1H\}$ 48.20 ppm [app. dt $J(HP_{1,3})$ = 12, $J(P_2P_{1,3})$ = 10, $J(RhP_{1,3})$ = 100 Hz, P_1 and P_3], 101.25 ppm [ddt $J(HP_2)$ = 36.5, $J(P_{1,3}P_2)$ = 10 Hz J(Rh) = 110 Hz, P_2]. These data suggest that oxidative addition of pentanal has occurred at the Rh^I centre. Unfortunately, this species has eluded definitive characterisation. It is tempting to speculate that whatever the underlying reasons behind the sluggish reactivity of **2a** with pentanal are, they are related to the formation of this stable hydride species.

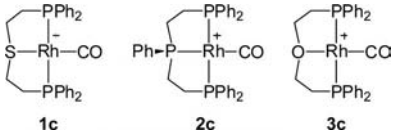

Scheme 5. ($[BAr^F_4]^-$ anions omitted for clarity).

The carbonyl species **1c**, **2c** and **3c** display CO stretches in their infrared spectra (CH_2Cl_2) characteristic of a single terminal CO ligand: **1c** 2021 cm^{-1}, **2c** 2029 cm^{-1},[8] **3c** 1995 cm^{-1}. The lower energy stretch seen in **3c** could be attributed to greater back-bonding to the CO π* orbital, mediated by stronger π donation by the O in the ligand to the metal centre. This is consistent with the upright geometry and observed bond lengths in **3a** in the solid state.

Reaction with Dichloromethane

[Rh{(κ^3-$Ph_2PCH_2CH_2)_2S$}Cl] reacts with CH_2Cl_2 over 18 h to give [Rh{(κ^3-$Ph_2PCH_2CH_2)_2S$}Cl_2CH_2Cl] (**1d**) (Scheme 6) in essentially quantitative yield, which was characterised by NMR spectroscopy and microanalysis. No intermediates were observed by $^{31}P\{^1H\}$ NMR spectroscopy. The $^{31}P\{^1H\}$ NMR spectrum of **1d** shows a doublet with a Rh–P coupling constant of 102 Hz, consistent with a Rh^{III} species. The ^{1}H NMR spectrum of the reaction with CD_2Cl_2 shows four methylene environments for the phosphane ligand, while the reaction with CH_2Cl_2 reveals an extra methylene environment (doublet of triplets) attributed to a CH_2Cl group. A *trans* chloride structure is proposed as the ^{1}H NMR spectrum shows only three phenyl proton environments, and a greater number of environments would be expected for isomers with lower symmetry (by assuming free rotation around the Rh–C bond). Oxidative addition of dichloromethane to Rh^I complexes is well documented.[43] Interestingly the analogous reaction with [Rh{(κ^3-$Ph_2PCH_2CH_2)_2PPh$}Cl] and dichloromethane was not observed at room temperature. This might be due to less available electron density on the metal centre [cf. ν(CO) **1c** 2021 cm^{-1} vs. **2c** 2029 cm^{-1}], although we currently only speculate upon this.

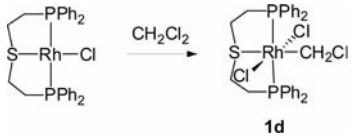

Scheme 6.

Conclusions

The Rh^I complexes [Rh{$(Ph_2PCH_2CH_2)_2E$}(alkene)]-[BAr^F_4] (alkene = methyl acrylate and trimethylvinylsilane) have been synthesised with the intention of studying their reactivity with simple aldehydes. The methyl acrylate ligands undergo a fluxional process on the metal, suggested to be via a κ^1-carbonyl intermediate, whereas the trimethylvinylsilane complexes cannot access this intermediate. Surprisingly, these complexes do not undergo reaction with pentanal at a reasonable rate, which is in contrast to reactions with chelating aldehydes containing a sulfur tether such as **A**. Presumably, this reflects the requirement for an intermediate with a coordinated σ-aldehyde to form prior to oxidative addition, and the alkene methylacrylate is too tightly bound to be displaced by pentanal. Irrespective of whether or not pentanal could be induced to undergo oxidative addition given the appropriate precursor complex, under catalytic conditions, the excess alkene will bind strongly to the metal centre thus attenuating reactivity with the aldehyde. Such sluggish reactivity has to be designed-out of future catalyst systems if non-chelating aldehydes are to be used in the hydroacylation reaction. We are currently exploring opportunities to do this.

Experimental Section

General: All procedures, unless otherwise stated, were carried out under an argon atmosphere, by using standard Schlenk-line and glove-box techniques. All glassware was dried at 130 °C overnight and flame-dried under vacuum before use. Dichloromethane, pentane and toluene were dried by using a Grubbs-type solvent purification system (MBraun SPS-800) and degassed by successive freeze-pump-thaw cycles before use.[44] CD_2Cl_2, fluorobenzene and benzene were dried with CaH_2, distilled under vacuum and stored over 3-Å molecular sieves. $(Ph_2PCH_2CH_2)_2S$,[27] $Na[BAr^F_4]$,[45] $[Rh(COD)Cl]_2$[46] and **3a**[21] were prepared according to literature methods. Methyl acrylate was distilled before use and degassed. All other chemicals were used as received by the supplier. NMR spectra were recorded on Bruker AVC 500, Varian Mercury 300 or Varian Unity 500 spectrometers at room temperature unless otherwise stated. Chemical shifts are quoted in ppm and coupling constants (J) in Hz. Residual protio solvent (e.g. CD_2Cl_2: δ = 5.32 ppm) was used as a reference for ^{1}H NMR spectroscopy. ESI-MS was carried out on a Bruker microTOF-Q connected to a glovebox (60 °C, 4.5 kV).[47] Infrared spectra were collected on a Nicolet Magna-I.R. 560 spectrometer. Elemental microanalysis was carried out by Stephen Boyer at London Metropolitan University. Elemental microanalysis was completed only on the crystalline samples of **2a** {as the $[B(3,5\text{-}Cl_2C_6H_3)_4]^-$ salt} and **1d**. The noncrystalline nature of the other samples inhibited accurate microanalysis. ESI mass spectrometry was attempted for all cationic complexes; however, in most cases a parent molecular ion was not observed.

X-ray crystallography data for **2a** (Table 1) were collected on an Enraf Nonius Kappa CCD diffractometer using graphite monochromated Mo-K_α radiation (λ = 0.71073 Å) and a low-temperature device [150(2) K];[48] data were collected using COLLECT, reduction and cell refinement were performed with DENZO/SCALEPACK.[49] The structure was solved by direct methods with SIR2004[50] and refined full-matrix least-squares on F^2 by using SHELXL-97.[51] All non-hydrogen atoms were refined with anisotropic displacement parameters. Alkene protons were located in the Fourier difference map; their isotropic displacement parameters were fixed to ride on the parent atoms. All other hydrogen atoms were placed in calculated positions by using the riding model. Disorder of the solvent molecule was treated by modelling it over two sites and restraining its geometry. Restraints to thermal parameters were applied where necessary in order to maintain sensible values. Because of the size of the crystals, data for **3a** (Table 1) were collected on I19 (EH1) at Diamond Light Source, Didcot. Data were collected at 150 K[48] with CrystalClear[52] and reduced using CrysAlisPro.[53] The structure was solved using SuperFlip[54] and refined with CRYSTALS.[55] On refinement, peaks were visible in the difference map close to the methyl acrylate, thus the occupancy was refined, and the peaks became more pronounced and clearly an alternative orientation was obtained with about 30% occupancy. Given the close proximity of the two components and their relative occupancies, free refinement was unstable, so "same-distance" restraints were used for the disordered components, and vibrational/thermal similarity restraints were used throughout. One phenyl ring of the anion had extremely prolate ellipsoids and was similarly modelled as disordered. Hydrogen atoms were generally visible in the difference map and were treated in the usual fashion,[56] positioned geometrically prior to refinement with soft restraints to give coordinates for use in a riding model with re-refinement as required. Torsion/dihedral angles were calculated with PLATON.[57] Crystallographic data have been deposited with the Cambridge Crystallographic Data Centre under CCDC-841412 (for **2a**) and -841413 (for **3a**). These data can be obtained free of charge from The Cambridge Crystallographic Data Centre via www.ccdc.cam.ac.uk/data_request/cif.

Table 1. Crystallographic data for **2a** and **3a**.

	2a·CH_2Cl_2	**3a**
Formula	$C_{63}H_{53}BCl_{10}O_2P_3Rh$	$C_{64}H_{46}BF_{24}O_3P_2Rh$
M_r	1403.18	1494.68
Crystal system	triclinic	monoclinic
Space group	$P\bar{1}$	$P2_1/c$
T [K]	150(2)	150(2)
a [Å]	11.85470(10)	13.8681(5)
b [Å]	16.2792(2)	28.8045(9)
c [Å]	16.6793(2)	16.6233(6)
α [°]	105.5233(5)	90
β [°]	94.1208(4)	106.893(3)
γ [°]	94.5998(5)	90
V [Å^3]	3076.82(6)	6353.9(4)
Z	2	4
Density [g cm^{-3}]	1.515	1.562
μ [mm^{-1}]	0.834	0.435
θ range [°]	$5.15 \leq \theta \leq 27.88$	$1.49 \leq \theta \leq 32.15$
Reflections collected	24620	85103
R_{int}	0.0228	0.135
Completeness	99.2%	96.0%
No. of data/restraints/parameters	14578/73/753	13243/1026/1578
R_1 [$I > 2\sigma(I)$]	0.0357	0.0643
wR_2 [all data]	0.0868	0.1509
GoF	1.039	0.9308
Largest diff. peak and hole [e Å^{-3}]	0.652, –0.658	1.25, –1.76

[Rh{(κ^3-$Ph_2PCH_2CH_2)_2S$}Cl]: $[Rh(COD)Cl]_2$ (50 mg, 0.101 mmol) was dissolved in toluene (6 mL) and heated to 60 °C in an oil bath. $(Ph_2PCH_2CH_2)_2S$ (93 mg, 0.203 mmol) was dissolved (using an ultrasound bath) separately in toluene (6 mL) and then slowly added dropwise to the hot stirring $[Rh(COD)Cl]_2$ solution. The solution changed colour to bright yellow/orange, followed by product precipitation. The solution was then cooled to –18 °C, and the resulting precipitate was filtered and washed with pentane. The precipitate was dried under vacuum to yield a very bright orange/yellow powder in 74% yield which was insoluble in benzene, fluorobenzene and acetone, and cleanly reacted with dichloromethane to give the C–Cl activated products **1d** (vide infra). NMR spectroscopic data were collected on a freshly prepared solution. ^{1}H NMR (300 MHz CD_2Cl_2): δ = 1.97 (td, J = 14, J = 5 Hz, 2 H, CH_2), 2.16 (t, J = 14 Hz, 2 H, CH_2), 3.00 (br. d, J = 13 Hz, 2 H, CH_2), 3.42 (br. t, J = 22 Hz, 2 H, CH_2), 7.28–7.45 (m, 12 H, Ph), 7.86–8.04 (m, 8 H, Ph) ppm. $^{31}P\{^1H\}$ NMR (122 MHz CD_2Cl_2): δ = 39.2 [d, J(RhP) = 147 Hz, 2 P] ppm.

[Rh{(κ^3-$Ph_2PCH_2CH_2)_2PPh$}Cl]: The synthesis was adapted from that of Marder and co-workers,[26] by following an analogous procedure as for the preparation of [Rh{(κ^3-$Ph_2PCH_2CH_2)_2S$}Cl] (above) to give a bright yellow micro-crystalline material (72% yield). The NMR spectroscopic data are in agreement with the published results.

[Rh{(κ^3-$Ph_2PCH_2CH_2)S$}(η^2-$H_2C{=}CHCOOCH_3$)][BAr^F_4] (1a): [Rh{(κ^3-$Ph_2PCH_2CH_2)_2S$}Cl] (9 mg, 0.015 mmol) was added to Na[BAr^F_4] (13.4 mg, 0.015 mmol) in a Young's NMR tube. To this was added methyl acrylate (13.5 μL, 0.150 mmol, 10 equiv.) and then CD_2Cl_2 (0.45 mL). A bright orange solution formed, which was concentrated to dryness under vacuum and washed with pentane (with sonication) three times. This was then dried under vacuum to yield an oily solid, which was characterised in situ by NMR spectroscopy. ^{1}H NMR (500 MHz CD_2Cl_2, 293 K): δ = 2.87 (m, 4 H, CH_2), 2.97–3.13 [m, 5 H, alkene(1 H) and CH_2 (4 H)], 3.23 (s, 3 H, CH_3), 3.83 (m, 1 H, alkene), 4.21 (m, 1 H, alkene), 7.46–7.69 (m, 20 H, Ph), 7.56 (s, 4 H, BAr^F_4), 7.73 (s, 8 H, BAr^F_4) ppm. $^{31}P\{^1H\}$ NMR (202 MHz CD_2Cl_2, 293 K): δ = 56.68 [d, J(RhP) = 126 Hz, 2 P] ppm. $^{31}P\{^1H\}$ NMR (202 MHz CD_2Cl_2, 200 K): tightly coupled AB double doublet, outer lines of very low intensity and could not be resolved. Inner lines: δ = 59.34 [d, J(RhP) = 129 Hz], 59.69 [d, J(RhP) = 129 Hz] ppm.

[Rh{(κ^3-$Ph_2PCH_2CH_2)S$}{η^2-$H_2C{=}CHSi(CH_3)_3$}][BAr^F_4] (1b): [Rh{(κ^3-$Ph_2PCH_2CH_2)_2S$}Cl] (9 mg, 0.015 mmol) was added to Na[BAr^F_4] (13.4 mg, 0.015 mmol) in a small Schlenk flask with a stirrer bar. To this was added vinyltrimethylsilane (22 μL, 0.150 mmol, 10 equiv.) and then CH_2Cl_2 (1 mL). The solution stirred for half an hour. The solvent was removed by vacuum, and the remaining yellow/brown oily solid was washed with pentane (with sonication) three times. After drying under vacuum, the complex was characterised in situ by NMR spectroscopy. ^{1}H NMR (500 MHz CD_2Cl_2, 293 K): δ = –0.41 (s, 9 H, $SiMe_3$), 1.85–3.75 (br., 8 H, CH_2), 3.10 [d, J(H,H)^{cis} = 12 Hz, 1 H, alkene(CH_2)], 3.88 [dd, J(H,H)^{trans} = 15 Hz, J(H,H)^{cis} = 6 Hz, 1 H, alkene(CHR)], 4.59 [m, 1 H, alkene (CH_2)], 7.33–7.61 (m, 20 H, Ph), 7.55 (s, 4 H, BAr^F_4), 7.73 (s, 8 H, BAr^F_4) ppm. $^{31}P\{^1H\}$ NMR (122 MHz CD_2Cl_2, 293 K): tightly coupled AB double doublet, outer lines of very low intensity and could not be resolved. Inner lines: δ = 54.97 [d, J(RhP) = 137 Hz], 57.72 [d, J(RhP) = 127 Hz] ppm. $^{31}P\{^1H\}$ NMR (202 MHz CD_2Cl_2, 200 K): δ = 55.21 [dd, J(P,P) = 282 Hz,

J(RhP) = 132 Hz, 1 P] 61.40 [dd, J(P,P) = 282 Hz, J(RhP) = 136 Hz, 1 P] ppm.

[Rh{(κ³-$Ph_2PCH_2CH_2$)S}CO][BAr^F_4] (1c): [Rh{(κ³-$Ph_2PCH_2CH_2$)$_2$S}Cl] (9 mg, 0.015 mmol) was added to Na[BAr^F_4] (13.4 mg, 0.015 mmol) in a Young's NMR tube. To this was added pentanal (13.4 μL, 0.126 mmol) and then CD_2Cl_2 (0.45 mL). The tube was shaken to encourage mixing to form a bright yellow solution. The resulting solution was then concentrated to dryness under vacuum and washed with pentane (with sonication) three times. After drying under vacuum, the product was characterised in situ by NMR spectroscopy. ^{1}H NMR (500 MHz CD_2Cl_2): δ = 2.58–3.79 (br., 8 H, CH_2), 7.47–7.69 (m, 20 H, Ph), 7.56 (s, 4 H, BAr^F_4), 7.73 (s, 8 H, BAr^F_4) ppm. ^{31}P{^{1}H} NMR (122 MHz CD_2Cl_2): δ = 53.34 [d, J(RhP) = 131 Hz, 2 P] ppm. IR (CH_2Cl_2): $\tilde{\nu}$ = 2021 cm^{-1}. ESI-MS: calcd. for [M$^+$] 589.04; found 589.04.

[Rh{(κ³-$Ph_2PCH_2CH_2$)S}Cl_2CH_2Cl] (1d): [Rh{(κ³-$Ph_2PCH_2CH_2$)$_2$S}Cl] (15 mg) was dissolved in CH_2Cl_2 and left for 18 h at 298 K. The complex was characterised in situ before the solution was layered with pentane to form a microcrystalline solid appropriate for microanalysis ^{1}H NMR (500 MHz CD_2Cl_2): δ = 2.85 (m, 2 H, CH_2), 3.27 (m, 2 H, CH_2), 3.40 (m, 2 H, CH_2), 3.82 (m, 4 H, CH_2 and CH_2Cl) 7.38–7.44 (m, 12 H, Ph), 7.74 (m, 4 H, Ph), 8.13 (m, 4 H, Ph) ppm. ^{31}P{^{1}H} NMR (122 MHz CD_2Cl_2): δ = 33.85 [d, J(RhP) = 102 Hz, 2 P] ppm.$C_{29}H_{30}Cl_3P_2SRh\cdot{}^1/_3CH_2Cl_2$ (710.14): calcd. C 49.61, H 4.35; found C 49.49, H 4.12.

[Rh{(κ³-$Ph_2PCH_2CH_2$)$_2$PPh}(η²-H_2C=CHCOOCH_3)][BAr^F_4] (2a): [Rh{(κ³-$Ph_2PCH_2CH_2$)$_2$PPh}Cl] (30 mg, 0.045 mmol) was added to Na[BAr^F_4] (39.6 mg, 0.045 mmol) in a small Schlenk flask. To this was added methyl acrylate (40 μL, 0.444 mmol, 10 equiv.) and then CH_2Cl_2 (1.5 mL). The solution was stirred for 1 h and filtered to remove NaCl. The resulting solution was concentrated to dryness under vacuum and washed with pentane (with sonication) three times before the resulting oil was dried under vacuum to form a yellow solid (yield = 52%). The solid-state structure was obtained by using the [B(3,5-$Cl_2C_6H_3$)$_4$]$^-$ salt, which was prepared by a similar method.[28] ^{1}H NMR (500 MHz CD_2Cl_2): δ = 2.10 (br., 2 H, CH_2), 2.27 (br., 2 H, CH_2), 2.60 (br., 2 H, CH_2), 2.91 [double multiplet, J(P,H) = 42 Hz, CH_2], 3.07 [d, J(H,H) = 6 Hz, 1 H, alkene(CH_2)], 3.13 (s, 3 H, CH_3), 4.04 [br., 2 H, alkene (coincident protons; CH_2 and CHCOOCH_3)], 7.3–7.65 (m, 25 H, Ph), 7.55 (s, 4 H, BAr^F_4), 7.73 (s, 8 H, BAr^F_4) ppm. ^{13}C{^{1}H} NMR (126 MHz CD_2Cl_2): δ = 27.48 (br., 2 C, CH_2), 32.75 (br., 2 C, CH_2), 52.01 (s, 1 C, CH_3), 71.74 (s, 1 C, alkene CH2), 72.67 (s, 1 C, alkene CHR), 128–134.5 (phenyl region + [BAr^F_4] resonances {118.16–117.94 (m), 125.16 [q, ^1J(F,C) = 272 Hz], 129.42 [qq, ^2J(F,C) = 31 Hz, ^4J(BC) = 3 Hz], 135.36 (s), 162.31 [q, ^1J(BC) = 50 Hz]}), 169.61 (s, 1 C, CO_2Me) ppm. ^{31}P{^{1}H} NMR (202 MHz CD_2Cl_2): δ = 66.49 [dd, J(P,P) = 38 Hz, J(RhP) = 132 Hz, 2 P], 123.29 [dt, J(P,P) = 38 Hz, J(RhP) = 134 Hz, 1 P] ppm. $C_{63}H_{53}BCl_{10}O_2P_3Rh\cdot CH_2Cl_2$ (1403.26) {as the [B(3,5-$Cl_2C_6H_3$)$_4$]$^-$ salt}: calcd. C 53.92, H 3.81; found C 54.45, H 3.96.

[Rh{(κ³-$Ph_2PCH_2CH_2$)$_2$PPh}{η²-H_2C=CHSi(CH_3)$_3$}][BAr^F_4] (2b): To [Rh{(κ³-$Ph_2PCH_2CH_2$)$_2$PPh}Cl] (10 mg, 0.015 mmol) was added Na[BAr^F_4] (13.2 mg, 0.015 mmol) and vinyltrimethylsilane (21.8 μL, 0.149 mmol) in CD_2Cl_2 (0.5 mL). This was agitated in an ultrasound bath for 1 h before in situ characterisation by NMR spectroscopy. ^{1}H NMR (500 MHz CD_2Cl_2): δ = –0.54 (s, 9 H, $SiMe_3$), 1.77–3.10 (br., 8 H, CH_2), 3.54 [d, J(H,H) = 12 Hz, 1 H, alkene (CH_2)], 4.55 [dd, J(H,H)^{trans} = 16 Hz, J(H,H)^{cis} = 10 Hz, 1 H, alkene(CHR)], 5.04 [br., 1 H, alkene (CH_2)], 7.35–7.69 (m, 25 H, Ph), 7.56 (s, 4 H, BAr^F_4), 7.74 (s, 8 H, BAr^F_4) ppm. ^{31}P{^{1}H} NMR (202 MHz CD_2Cl_2): δ = 55.03 [ddd, J(RhP) = 138 Hz, J(P,P)^{cis} = 34 Hz, J(P,P)^{trans} = 240 Hz, 1 P], 63.05 [ddd, J(RhP) = 132 Hz, J(P,P)^{cis} = 37 Hz, J(P,P)^{trans} = 240 Hz, 1 P], 115.18 [dt, J(RhP) = 142 Hz, J(P,P) = 35 Hz, 1 P] ppm.

[Rh{(κ³-$Ph_2PCH_2CH_2O$}CO][BAr^F_4] (3c): To the best of our knowledge, no NMR or IR data has been reported for this known species, hence we report it here.[35] (NMR tube scale) Compound **3a** (10 mg, 0.015 mmol) was dissolved in [D_6]acetone and to this was added pentanal (7.1 μL, 0.067 mmol). The sealed tube was hydrogenated under H_2 (4 atm). After 48 h, the carbonyl species forms as the sole product and was characterised in situ by NMR and IR spectroscopy and ESI mass spectrometry. ^{31}P{^{1}H} NMR (122 MHz [D_6]acetone): δ = 49.67 [d, J(RhP) = 129 Hz, 2 P] ppm. IR ([D_6]acetone): $\tilde{\nu}$ = 1995 cm^{-1}. ESI-MS: calcd. for [M$^+$] 573.06; found 573.06.

Acknowledgments

The EPSRC and the University of Oxford are acknowledged for support.

[1] D. P. Fairlie, B. Bosnich, *Organometallics* **1988**, *7*, 946–954.
[2] J. W. Suggs, *J. Am. Chem. Soc.* **1978**, *100*, 640–641.
[3] M. C. Willis, *Chem. Rev.* **2010**, *110*, 725–748 .
[4] T. B. Marder, D. C. Roe, D. Milstein, *Organometallics* **1988**, *7*, 1451–1453.
[5] Z. Shen, P. K. Dornan, H. A. Khan, T. K. Woo, V. M. Dong, *J. Am. Chem. Soc.* **2009**, *131*, 1077–1091.
[6] A. H. Roy, C. P. Lenges, M. Brookhart, *J. Am. Chem. Soc.* **2007**, *129*, 2082–2093.
[7] I. F. D. Hyatt, H. K. Anderson, A. T. Morehead, A. L. Sargent, *Organometallics* **2008**, *27*, 135–147.
[8] C. M. Beck, S. E. Rathmill, Y. J. Park, J. Chen, R. H. Crabtree, L. M. Liable-Sands, A. L. Rheingold, *Organometallics* **1999**, *18*, 5311–5317.
[9] P. Fristrup, M. Kreis, A. Palmelund, P.-O. Norrby, R. Madsen, *J. Am. Chem. Soc.* **2008**, *130*, 5206–5215.
[10] A. T. Luedtke, K. I. Goldberg, *Inorg. Chem.* **2007**, *46*, 8496–8498.
[11] M. P. Lanci, M. S. Remy, D. B. Lao, M. S. Sanford, J. M. Mayer, *Organometallics* **2011**, *30*, 3704–3707.
[12] D. Milstein, *Acc. Chem. Res.* **1984**, *17*, 221–226.
[13] R. Goikhman, D. Milstein, *Angew. Chem.* **2001**, *113*, 1153; *Angew. Chem. Int. Ed.* **2001**, *40*, 1119–1122.
[14] C. H. Jun, E. A. Jo, J. W. Park, *Eur. J. Org. Chem.* **2007**, 1869–1881.
[15] K. Tanaka, Y. Shibata, T. Suda, Y. Hagiwara, M. Hirano, *Org. Lett.* **2007**, *9*, 1215–1218.
[16] M. M. Coulter, K. G. M. Kou, B. Galligan, V. M. Dong, *J. Am. Chem. Soc.* **2010**, *132*, 16330–16333.
[17] M. C. Willis, S. J. McNally, P. J. Beswick, *Angew. Chem.* **2004**, *116*, 344; *Angew. Chem. Int. Ed.* **2004**, *43*, 340–343.
[18] J. C. Jeffrey, T. B. Rauchfuss, *Inorg. Chem.* **1979**, *18*, 2658–2666.
[19] G. L. Moxham, H. E. Randell-Sly, S. K. Brayshaw, R. L. Woodward, A. S. Weller, M. C. Willis, *Angew. Chem.* **2006**, *118*, 7780; *Angew. Chem. Int. Ed.* **2006**, *45*, 7618–7622.
[20] G. L. Moxham, H. Randell-Sly, S. K. Brayshaw, A. S. Weller, M. C. Willis, *Chem. Eur. J.* **2008**, *14*, 8383–8397.
[21] R. J. Pawley, G. L. Moxham, R. Dallanegra, A. B. Chaplin, S. K. Brayshaw, A. S. Weller, M. C. Willis, *Organometallics* **2010**, *29*, 1717–1728.
[22] K. Wang, T. J. Emge, A. S. Goldman, C. Li, S. P. Nolan, *Organometallics* **1995**, *14*, 4929–4936.
[23] J. F. Riehl, Y. Jean, O. Eisenstein, M. Pelissier, *Organometallics* **1992**, *11*, 729–737.
[24] M. Kreis, A. Palmelund, L. Bunch, R. Madsen, *Adv. Synth. Catal.* **2006**, *348*, 2148–2154.

[25] M. A. Garralda, *Dalton Trans.* **2009**, 3635–3645.
[26] S. A. Westcott, G. Stringer, S. Anderson, N. J. Taylor, T. B. Marder, *Inorg. Chem.* **1994**, *33*, 4589–4594.
[27] G. Degischer, G. Schwarzenbach, *Helv. Chim. Acta* **1966**, *49*, 1927–1931.
[28] A. B. Chaplin, A. S. Weller, *Eur. J. Inorg. Chem.* **2010**, 5124–5128.
[29] E. Hauptman, S. Sabo-Etienne, P. S. White, M. Brookhart, J. M. Garner, P. J. Fagan, J. C. Calabrese, *J. Am. Chem. Soc.* **1994**, *116*, 8038–8060.
[30] R. Bender, C. Okio, R. Welter, P. Braunstein, *Dalton Trans.* **2009**, 4901–4907.
[31] A. J. Edwards, S. Elipe, M. A. Esteruelas, F. J. Lahoz, L. A. Oro, C. Valero, *Organometallics* **1997**, *16*, 3828–3836.
[32] T. A. Albright, R. Hoffmann, J. C. Thibeault, D. L. Thorn, *J. Am. Chem. Soc.* **1979**, *101*, 3801–3812.
[33] M. Rubio, A. Suarez, D. del Río, A. Galindo, E. Ålvarez, A. Pizzano, *Organometallics* **2009**, *28*, 547–560.
[34] C. Daniel, N. Koga, J. Han, X. Y. Fu, K. Morokuma, *J. Am. Chem. Soc.* **1988**, *110*, 3773–3787.
[35] N. W. Alcock, J. M. Brown, J. C. Jeffery, *J. Chem. Soc., Dalton Trans.* **1976**, 583–588.
[36] U. Helmstedt, P. Lönnecke, E. Hey-Hawkins, *Inorg. Chem.* **2006**, *45*, 10300–10308.
[37] X. Shan, J. H. Espenson, *Organometallics* **2003**, *22*, 1250–1254.
[38] E. W. Abel, M. Booth, K. G. Orrell, G. M. Pring, *J. Chem. Soc., Dalton Trans.* **1981**, 1944–1950.
[39] R. Sustmann, B. Patzke, R. Boese, *J. Organomet. Chem.* **1994**, *470*, 191–197.
[40] D. Kwon, M. D. Curtis, *Organometallics* **1990**, *9*, 1–5.
[41] B. K. Corkey, F. L. Taw, R. G. Bergman, M. Brookhart, *Polyhedron* **2004**, *23*, 2943–2954.
[42] D. P. Fairlie, B. Bosnich, *Organometallics* **1988**, *7*, 936–945.
[43] A. J. Vetter, R. D. Rieth, W. W. Brennessel, W. D. Jones, *J. Am. Chem. Soc.* **2009**, *131*, 10742–10752 and references therin.
[44] A. B. Pangborn, M. A. Giardello, R. H. Grubbs, R. K. Rosen, F. J. Timmers, *Organometallics* **1996**, *15*, 1518–1520.
[45] W. E. Buschmann, J. S. Miller, K. Bowman-James, C. N. Miller, *Inorg. Synth.* **2002**, *33*, 83–85.
[46] G. Giordano, R. H. Crabtree, *Inorg. Synth.* **1990**, *28*, 88–90.
[47] A. T. Lubben, J. S. McIndoe, A. S. Weller, *Organometallics* **2008**, *27*, 3303–3306.
[48] J. Cosier, A. M. Glazer, *J. Appl. Crystallogr.* **1986**, *19*, 105–107.
[49] Z. Otwinowski and W. Minor in *Processing of X-Ray Diffraction Data Collected in Oscillation Mode*, Vol. 276 **1997**, pp. 307–326.
[50] M. C. Burla, R. Caliandro, M. Camalli, B. Carrozzini, G. L. Cascarano, L. De Caro, C. Giacovazzo, G. Polidori, R. Spagna, *J. Appl. Crystallogr.* **2005**, *38*, 381–388.
[51] G. M. Sheldrick, *Acta Crystallogr., Sect. A* **2008**, *64*, 112–122.
[52] *CrystalClear*, Rigaku Americas and Rigaku Corporation, **2009**.
[53] *CrysAlisPro*, Oxford Diffraction/Agilent Technologies, **2010**.
[54] L. Palatinus, G. Chapuis, *J. Appl. Crystallogr.* **2007**, *40*, 786–790.
[55] P. W. Betteridge, J. R. Carruthers, R. I. Cooper, K. Prout, D. J. Watkin, *J. Appl. Crystallogr.* **2003**, *36*, 1487.
[56] R. I. Cooper, A. L. Thompson, D. J. Watkin, *J. Appl. Crystallogr.* **2010**, *43*, 1100–1107.
[57] A. L. Spek, *J. Appl. Crystallogr.* **2003**, *36*, 7–13.

Received: September 8, 2011
Published Online: November 14, 2011

